Regular Article

Dual functionality of vibration attenuation and energy harvesting: effect of gradation on non-linear multi-resonator metastructures

A. Chaurha[1], P. V. Malaji[2], and T. Mukhopadhyay[1,a]

[1] Department of Aerospace Engineering, Indian Institute of Technology Kanpur, Kanpur, India
[2] Vibration, Energy Harvesting and IoT Lab, BLDEA's V. P. Dr. P. G. Halakatti College of Engineering and Technology, Vijayapur, India

Abstract Metastructures and phononic crystals could have several unique physical properties, such as effective negative parameters, tunable band gaps, negative refraction, and so on, which allow them to improve multi-physical performances at the materials level. Motivated by the elastic negative mass metastructures, this work reports the enhancement of bandwidth and vibration suppression while achieving better energy harvesting via non-linear attachments. We propose to consider the effect of spring softening and spring hardening simultaneously along with exploiting the coupled influence of multiple variables, such as spring stiffness, damping, number of unit cells, electro-mechanical coupling coefficient and masses. A mathematical model of the metastructure having linear spring with nonlinear attachments is developed and analyzed numerically including the effect of functional gradation. Dimensionless parametric study is performed to tune two-cell and multi-cell models to enhance vibration suppression and energy harvesting performances. In an eight-cell model, the non-linear characteristic parameter is functionally graded from softening to hardening using exponential and power law to explore the dual functionality further. It is revealed that the resonant peak can be reduced by non-linear softening characteristics. For enhanced energy harvesting, a smaller value of mass ratio is preferred, while a larger value of damping characteristic is suitable for vibration suppression. Under certain configurations, band structure of the phononic metastructure is capable of achieving absolute band gaps, resulting in frequency ranges, where waves cannot propagate. The comprehensive analysis presented here on the effect of various system parameters would lead to the design of non-linear multi-resonator metamaterials for the dual functionality of vibration attenuation and energy harvesting that can be applied in a wide range of automated systems and self-powered devices including the capabilities of real-time monitoring and active behaviour.

1 Introduction

Vibration problems have significant impacts on a wide range of engineering applications including civil, aerospace and mechanical engineering, where vibration and dynamic loading conditions are frequently encountered. When a structure or component of equipment is exposed to periodic movements, vibrations are observed. The vibration and resulting resonance effects can generate extreme stresses leading to extreme deformations of structure, which further can lead to failure of structures in some cases. As a result, vibration analysis is an important aspect of structural designs to ensure safety and serviceability. For example, resonance in aircraft wings needs to be eliminated, as it could drastically affect the flight conditions. Tall buildings and bridges are subjected to the large amplitude of vibration due to wind, earthquakes, water waves, and vehicle movements. The Tacoma Narrows Bridge collapsed in 1940 as a result of resonance due to the wind [1], which highlights the importance of appropriate dynamic analysis and design.

In a conventional energy harvesting system, a single mechanical resonance peak can amplify the amplitude of vibration that can be used to convert mechanical energy to electrical energy. Although natural frequency can amplify the mechanical vibration amplitude for a frequency domain but other than natural mode, it can affect the energy harvesting performance. In addition, we can adjust the natural frequency and size of the natural frequency peak by changing the limited design parameters, but other effective characteristics for energy harvesting such as the width and shape of the peak are difficult to be fine-tuned.

In the last few years, the concept of mechanical metamaterial has come to light that gives rare and unexpected properties, which are not found in tradi-

[a] e-mail: tanmoy@iitk.ac.in (corresponding author)

1404

Eur. Phys. J. Spec. Top. (2022) 231:1403–1413

tional materials, due to adoption of rationally designed material architectures [2–9]. In comparison to natural materials, metamaterials exhibit unprecedented innovative capabilities and promising application potentials to meet the modern multi-functional structural demands. Elastic mechanical metamaterials can exhibit unconventional physical properties, such as negative mass and negative stiffness for a specified frequency range. Huang et al. [10] demonstrated and compared various similar models to showcase the structures consisting of mass in the mass system. They discovered that the effective mass density of mass in a mass lattice system varies with frequency and at the resonance of inner mass, effective density could be negative. Huang et al. [11] and Li et al. [12] presented an acoustic metamaterial with a negative mass density and negative Young's modulus simultaneously. Cheng et al. [13] showed that one-dimensional structured ultrasonic metamaterials can exhibit both negative effective mass and bulk modulus simultaneously for specific frequency ranges. Yang et al. [14] presented experimentally and theoretically that membrane-type acoustic metamaterials show negative dynamic mass at a frequency around the total reflection frequency. Recently Mukhopadhyay and Adhikari have presented analytical and experimental investigations for 2D lattice-type metamaterials showing extreme modulation of effective elastic moduli under dynamic condition, including attainment of the negative values at certain critical frequency ranges [15–18].

Bandgap is the ability of materials to restrict the wave transmission over a specified frequency range. Reynolds et al. [19] presented a new form of viscoelastic metamaterial that can be used as highly efficient vibration isolator at a lower frequency range. A mathematical analysis was carried out to develop a prototype for manipulating the bandgap. Conventionally tuned mass dampers generate narrow bandwidth frequency, but in the mechanical metamaterials the band width can be increased widely by tuning the system parameters. Distinctive bandgap of structures results in better vibration isolation and energy harvesting performance [20]. Huang et al. [21] proposed mass in mass lattice system with multiple resonator acoustic metamaterial to attain multiple band gaps. They reported that major bandgaps are achieved by the outer mass. A phononic medium is a type of structure which exhibits some form of periodicity in terms of material, geometry or boundary condition. Hussein et al. [22] presented the historical development of dynamic, vibration, and acoustic response of the phononic structure. Nonlinear energy sinks use smaller mass as compared to vibration absorber and widen the frequency range to minimize vibrations [23,24]. Broad bandwidth can be achieved by introducing non-linearity in energy harvesters. The bandwidth of a device can be increased by the non-linear energy harvester due to the hardening and softening responses [25]. Cottone et al. [26] enhanced the performance of standard linear oscillators by exploitation of non-linear oscillators. Xia et al. [27] proposed enhancement of frequency bandwidth in locally resonant metamaterial based finite structure

via bi-stable attachments. Lazarov et al. [28] investigated the dynamic characteristics of one dimensional chain with nonlinear oscillators and analysed the band gap shift in linear and non-linear systems. Xia et al. [29] showed the transition from linear locally resonant bandgaps to non-linear regimes. Enhancement of bandwidth can be observed in cantilever beams under base excitation with non-linear attachment. Banerjee et al. [30] numerically investigated the effect of applying two main classes of duffing type cubic non-linearity named mono-stable and bi-stable on the attenuation bandwidth of an elasto-dynamic metamaterial. They found that the bandwidth of a bi-stable non-linear system is 2–3 times wider than the equivalent linear system and in the case of mono-stable system bandwidth does not change a lot. Concerning the increase in vibration attenuation bandwidth of metastructures, linear spring, non-linear spring, damper, electro-mechanical transducer are found to affect the dynamic response in literature [28,31,32].

Metastructures for vibration mitigation can be simultaneously used for energy harvesting [33–35]. Piezoelectric materials have the ability to convert mechanical strain energy into electrical voltage and vice versa [36–38]. Piezoelectric and electromagnetic conversion methods are most commonly used to convert mechanical energy into electrical voltage [39,40]. The produced electrical power can be used to operate the sensors for health monitoring and a range of low-power automation devices [41], covering applications in the fields of structural monitoring, medical implants and industrial automation. Figure 1 presents an introductory overview of vibration isolation, energy harvesting and general application of mechanical metamaterials. Sodano et al. [42] provided a review on recent research on power harvesting using piezoelectric materials. Tang et al. [43] presented multiple models for multiple degrees of freedom piezoelectric energy harvesting modes. They analyzed different models and tuned the models to enhance energy harvesting performance. Erturk et al. [44] developed a vibration-based piezoelectric generator, with detailed investigation on modelling, design and optimization of power generation. Carrara et al. [39] used three concepts covering wave focusing, energy localization and wave guiding to develop metamaterials for improved energy harvesting. It was shown that the metamaterial energy harvesting system can increase the power by many orders of magnitude.

The linear resonators have shown narrow-banded performance from vibration attenuation and energy harvesting point of view [45]. The nonlinear characteristics in energy harvesting have shown significant enhancement of energy output efficacy [42,44]. Similar effects can be observed when nonlinear resonators are used in metastructure for vibration attenuation [29]. Rezaei et al. explored possibilities of vibration attenuation and energy harvesting with bistable absorber [46]. They reported enhancement in both vibration attenuation and energy harvesting efficiency. The recent years have witnessed that a better vibration reduction and simultaneous vibration energy harvesting can
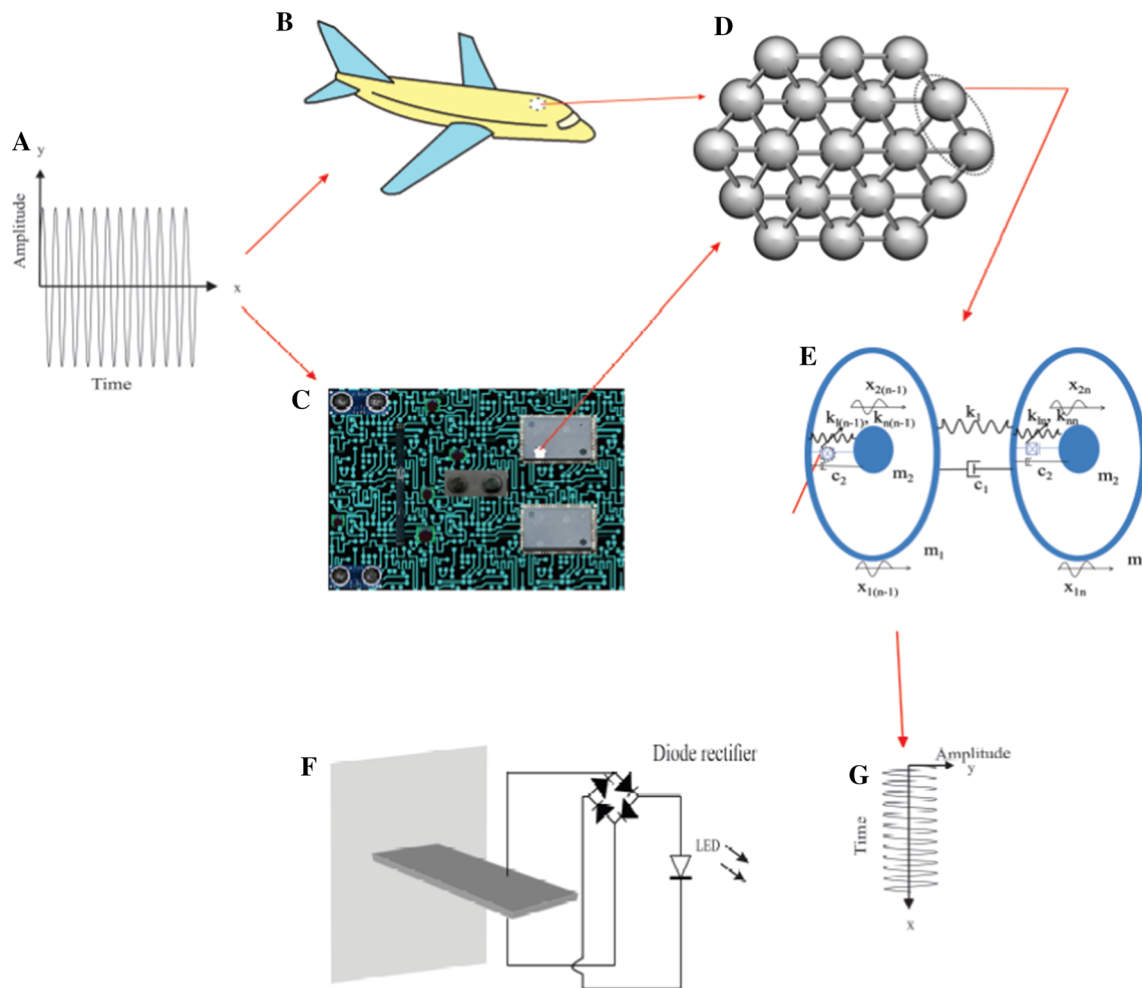
Fig. 1 Overview of the dual functionality of vibration attenuation and energy harvesting in metamaterials. **A** Typical representation of high amplitude mechanical waves encountered by structures. **B** Structures vulnerable to high amplitude vibration. **C** Sensors which operate in the vibration environment. **D** Typical representation of phononic metamaterial structure. **E** A metamaterial with negative density. **F** Energy harvesting circuit that is embedded in the unit cell. **G** Low amplitude mechanical waves as an output of the metamaterial. Due to the specific structure of negative density metamaterials, high amplitude mechanical waves can be modified to low amplitude waves and subsequently the potential of energy harvesting using the vibrational energy can also be enhanced. Due to such dual functionality, these metamaterials have potential applications in vibration mitigation while enabling the manufactured self-power devices for health monitoring and real-time interrogation of various operation features

be achieved by inducing nonlinearity. Many of the literature have considered metastructures with repeated similar nonlinear resonators for vibration attenuation and energy harvesting [33]. These resonators usually exhibit either softening or hardening characteristics. In this paper, we aim to consider resonators with spring softening and spring hardening and combination of both softening and hardening effect with different linear natural frequencies to understand the effect on vibration attenuation and energy harvesting. A careful review of literature in the field of dynamic metamaterials reveals that the dual functionality of maximizing vibration attenuation and energy harvesting simultaneously is challenging due to their contradictory demands in terms of vibration amplitude. Here we aim to address this aspect of dual functionality based on negative density metastructures, which have a poten-

tial to enhance the vibration attenuation and energy harvesting performance by introducing nonlinear spring in inner mass (softening and hardening spring) of the unit cell, and exploiting the coupled influence of multiple variables, such as spring stiffness, damping, number of unit cells, electro-mechanical coupling coefficient and masses. Hereafter in this paper, Sect. 2 presents system mathematical models and equations for the metamaterial, Sect. 3 presents numerical simulation results and brief discussion of the outcomes, and finally, conclusions of the current work is provided in Sect. 4.

2 Non-linear metamaterial model

Figure 2A represents negative mass metamaterial multi-cell model with piezoelectric transducer. Negative den-
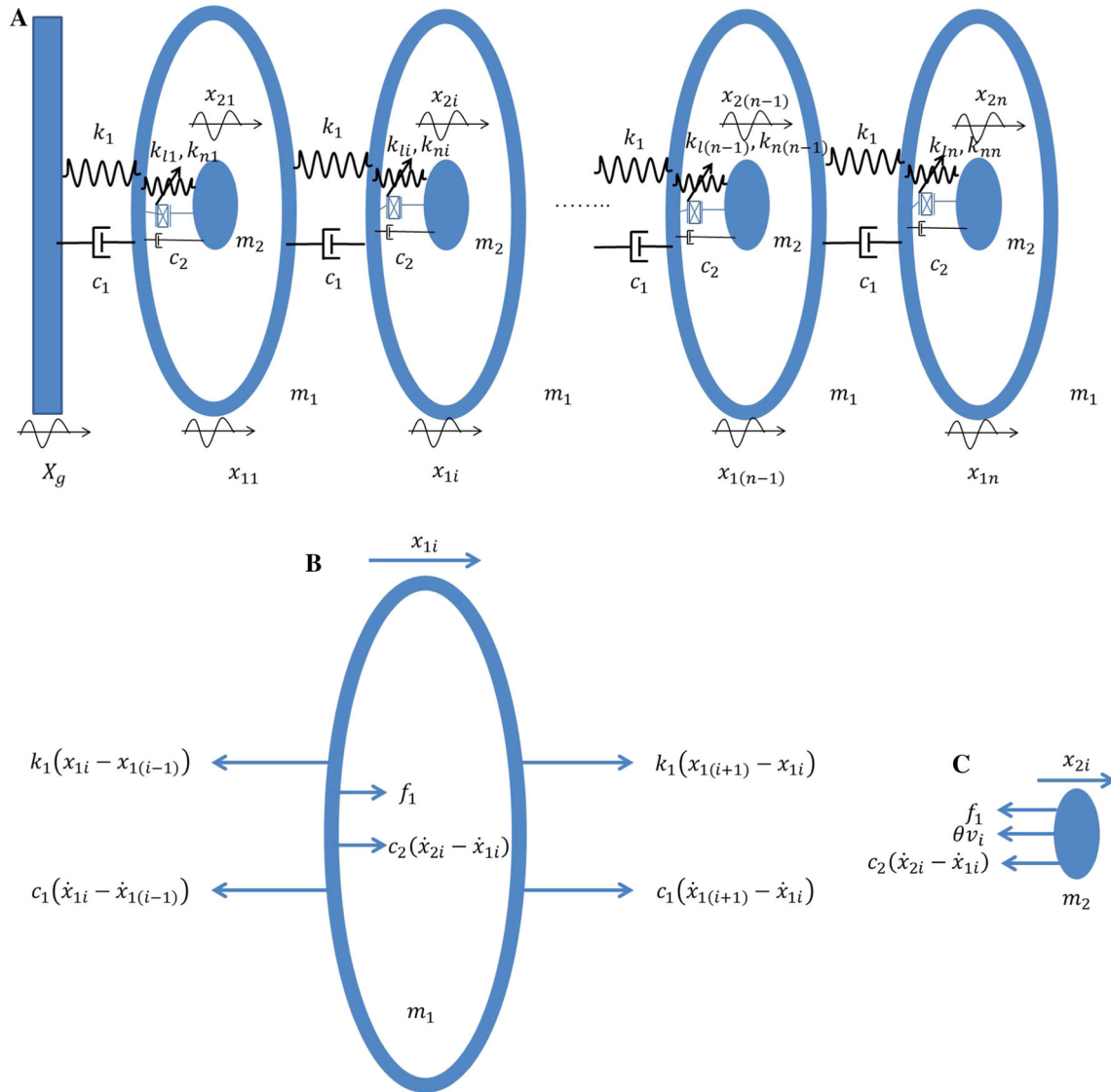
Fig. 2 Multi-cell metastructure model. **A** The proposed metamaterial has two masses in each unit cell, where vibration of the in-cell masses is responsible for energy harvesting and the amplitude of primary mass for the last unit cell nor- mally contributes to the aspect of vibration mitigation. **B** Free body diagram (FBD) of outer mass (m_1). **C** FBD of inner mass (m_2), where $f_1 = k_{li}(x_{2i} - x_{1i}) + k_{ni}(x_{2i} - x_{1i})^3$

sity metastructure is referred to as a mass-in-mass system which can be mathematically modeled as an outer sphere having mass (m_1) connected with an inner sphere of mass (m_2) with non-linear spring, damper and energy harvesting devices. The primary system is considered as a chain of linear spring (k_1), damper (c_1) and mass (m_1) system. Each main mass (m_1) consists of local nonlinear resonator with nonlinear spring (linear stiffness k_{li} and nonlinear cubic stiffness k_{ni}), damping (c_2) and inner mass (m_2). These resonators are attached to piezoelectric patches for energy harvesting with electro-mechanical coupling coefficient (θ), capacitance (C) and resistance (R). The system is subjected to harmonic base excitation $X_g\cos(\omega t)$. The voltage generated by a unit cell is v_i. Figure 2B represents the free body diagram of outer mass m_1 and Fig. 2C

represents the free body diagram of inner mass m_2. Under the dynamic condition, the governing equations of motion for the ith element are

$$
\begin{aligned}
m_1\ddot{x}_{1i} \; &+c_1(-\dot{x}_{1(i-1)} + 2\dot{x}_{1i} - \dot{x}_{1(i+1)}) \\
&+c_2(\dot{x}_{1i} - \dot{x}_{2i}) + k_1(-x_{1(i-1)} \\
&+2x_{1i} - x_{1(i+1)}) + k_{li}(x_{1i} - x_{2i}) \\
&+k_{ni}(x_{1i} - x_{2i})^3 - \theta v_i = 0 \quad (1)
\end{aligned}
$$

$$
\begin{aligned}
m_1\ddot{x}_{1n} \; &+c_1(-\dot{x}_{1(n-1)} + \dot{x}_{1n}) + c_2(\dot{x}_{1n} \\
&-\dot{x}_{2n}) + k_1(-x_{1(n-1)} \\
&+x_{1n}) + k_{ln}(x_{1n} - x_{2n}) + k_{ni}(x_{1n} \\
&-x_{2n})^3 - \theta v_n = 0 \quad (2)
\end{aligned}
$$

$$m_2\ddot{x}_{2i} \; + c_2(\dot{x}_{2i} - \dot{x}_{1i}) + k_{li}(x_{2i} - x_{1i})$$
$$+ k_{ni}(x_{2i} - x_{1i})^3 + \theta v_i = 0 \tag{3}$$
$$\frac{v_i}{R} + C\dot{v}_i + \theta(\dot{x}_{2i} - \dot{x}_{1i}) = 0 \tag{4}$$

The value of nonlinear cubic stiffness can be changed to get spring hardening ($k_{ni} > 0$) and spring softening ($k_{ni} < 0$) effects. The non dimensional form of the above electro-mechanical equations are given as

$$\ddot{X}_{1i} \; + \zeta_1(-\dot{X}_{1(i-1)} + 2\dot{X}_{1i} - \dot{X}_{1(i+1)})$$
$$+ \zeta_2\Gamma_{li}\mu(\dot{X}_{1i} - \dot{X}_{2i}) + (-X_{1(i-1)}$$
$$+ 2X_{1i} - X_{1(i+1)})$$
$$+ \Gamma_{li}{}^2\mu(X_{1i} - X_{2i}) + \lambda_{ni}\Gamma_{li}{}^2\mu(X_{1i}$$
$$- X_{2i})^3 - \mu\Gamma_{li}{}^2\beta V_i = 0 \tag{5}$$
$$\ddot{X}_{1n} \; + \zeta_1(-\dot{X}_{1(n-1)} + \dot{X}_{1n})$$
$$+ \zeta_2\Gamma_{ln}\mu(\dot{X}_{1n} - \dot{X}_{2n}) + (-X_{1(n-1)}$$
$$+ X_{1n}) + \Gamma_{ln}{}^2\mu(X_{1n} - X_{2n})$$
$$+ \lambda_{nn}\Gamma_{ln}{}^2\mu(X_{1n}$$
$$- X_{2n})^3 - \mu\Gamma_{ln}{}^2\beta V_n = 0 \tag{6}$$
$$\ddot{X}_{2i} \; + \zeta_2\Gamma_{li}(\dot{X}_{2i} - \dot{X}_{1i}) + \Gamma_{li}{}^2(X_{2i} - X_{1i})$$
$$+ \lambda_{ni}\Gamma_{li}{}^2(X_{2i} - X_{1i})^3 + \Gamma_{li}{}^2\beta V_i = 0 \tag{7}$$
$$\dot{V}_i + \eta V_i + \kappa(\dot{X}_{2i} - \dot{X}_{1i}) = 0 \tag{8}$$

where the non dimensional parameters are defined as

$$\zeta_1 = \frac{c_1}{m_1\omega_1}, \quad \zeta_2 = \frac{c_2}{m_2\omega_{2i}}, \quad \Gamma_{li} = \frac{\omega_{2i}}{\omega_1}, \quad \lambda = \frac{k_{ni}}{k_{li}}$$
$$\mu = \frac{m_2}{m_1}, \quad \omega_1 = \sqrt{\frac{k_1}{m_1}}, \quad \Omega = \frac{\omega}{\omega_1}, \quad \beta = \frac{\theta}{k_{li}}$$
$$\kappa = \frac{\theta}{C}, \quad \eta = \frac{1}{CR\omega_1}, \quad \omega_{2i} = \sqrt{\frac{k_{li}}{m_2}} \tag{9}$$

The parameter $\tau \; (= \omega_1 t)$ represents non-dimensional time. For the first unit cell $x_{1(i-1)}$ is harmonic base excitation $X_g\cos(\omega t)$. Here a Matlab based ODE solver is used to solve the time domain equations by neglecting the transient effect of the dynamic system and analysing the steady state response considering the last 25% time length.

The scope of the present work is to design a metastructure to mitigate vibration and harvest energy for a source, where frequency cannot be measured exactly. Under such circumstances, metastructure should be capable of mitigating vibration and harvesting enough power within a known range of frequencies. The manuscript presents a study to understand the effect of spring softening, hardening, electromechanical coupling and number of unit cells on the vibration mitigation and energy harvesting efficacy subjected to harmonic base excitation. However, in practice, the structures are subjected to random (noise) excitations rather than harmonic excitations (not within the scope of the current

paper). Thus, it would be interesting to see the effect of noise magnitude on the dual performance criteria including nonlinear oscillator for potential well escape which in turn influences the dual functionality. The current development would work as the baseline reference for such future studies.

3 Results and discussion

In the mass in mass metamaterials at the resonance frequency, the internal mass response is much larger as compared to the outer mass response. In a particular frequency bandgap more than the resonance frequency of internal mass, for the given excitation, internal mass shows out of phase response. Subsequently, for a unit cell total movement becomes out of phase. This situation can be represented by negative mass to the equivalent single degree of freedom system. Therefore, mass in mass resonating material is called a negative mass metamaterial. For a multi-cell metamaterial effective properties of the system depend on the local resonance of unit cells and out of phase motion of different unit cells. Locally units of the metastructure can be able to form bandgap for a wavelength higher than the lattice length of a unit. The bandgap of metastructure can be varied by changing the natural frequency locally. The specifically designed metamaterials can modulate the wave transmission via dynamic physical properties. In the attenuation bandgap, energy can not transfer through the metamaterial and major energy flows in the in-cell resonating masses causing their high amplitude response. Therefore, by applying an energy harvesting system with the in-cell mass, energy can be converted effectively from vibration energy to electrical energy. This would serve the dual functionality of vibration attenuation and energy harvesting. In the subsequent paragraphs, we present numerical results on multi-cell mass in mass metamaterials including the effect of non-linearity.

We start our analysis by considering a 2-cell system (with 4 degrees of freedom) and investigate the coupled influence of different system parameters, as presented in Fig. 3. The following parameters are used for obtaining the numerical results unless otherwise mentioned: $\zeta_1 = 0.03$, $\zeta_2 = 0.1$, $\mu = 0.2$, $\eta = 1$, $\kappa = \beta = 0.05$. Figure 3A, B assumes the non-dimensional parameters as $X_g = 0.1$ and $\Gamma_{l1} = \Gamma_{l2} = 0.61$ under a steady state condition. Figure 3A represents the non-dimensional steady-state RMS amplitude of the first mass (m_1) of last unit cell for different combinations of softening and hardening coefficient (λ). We are getting double valley phenomena, in which the first peak is having a higher amplitude as compared to the second peak. Enhancement of bandwidth will be found by the multi-valley phenomena due to the presence of multi-degree of freedom. For both cells having hardening coefficient ($\lambda_1 = 0.1$, $\lambda_2 = 0.1$), we obtain largest RMS amplitude of first peak. As we introduce softening coefficient in both unit cells ($\lambda_1 = -0.1$, $\lambda_2 = -0.1$), lowest RMS
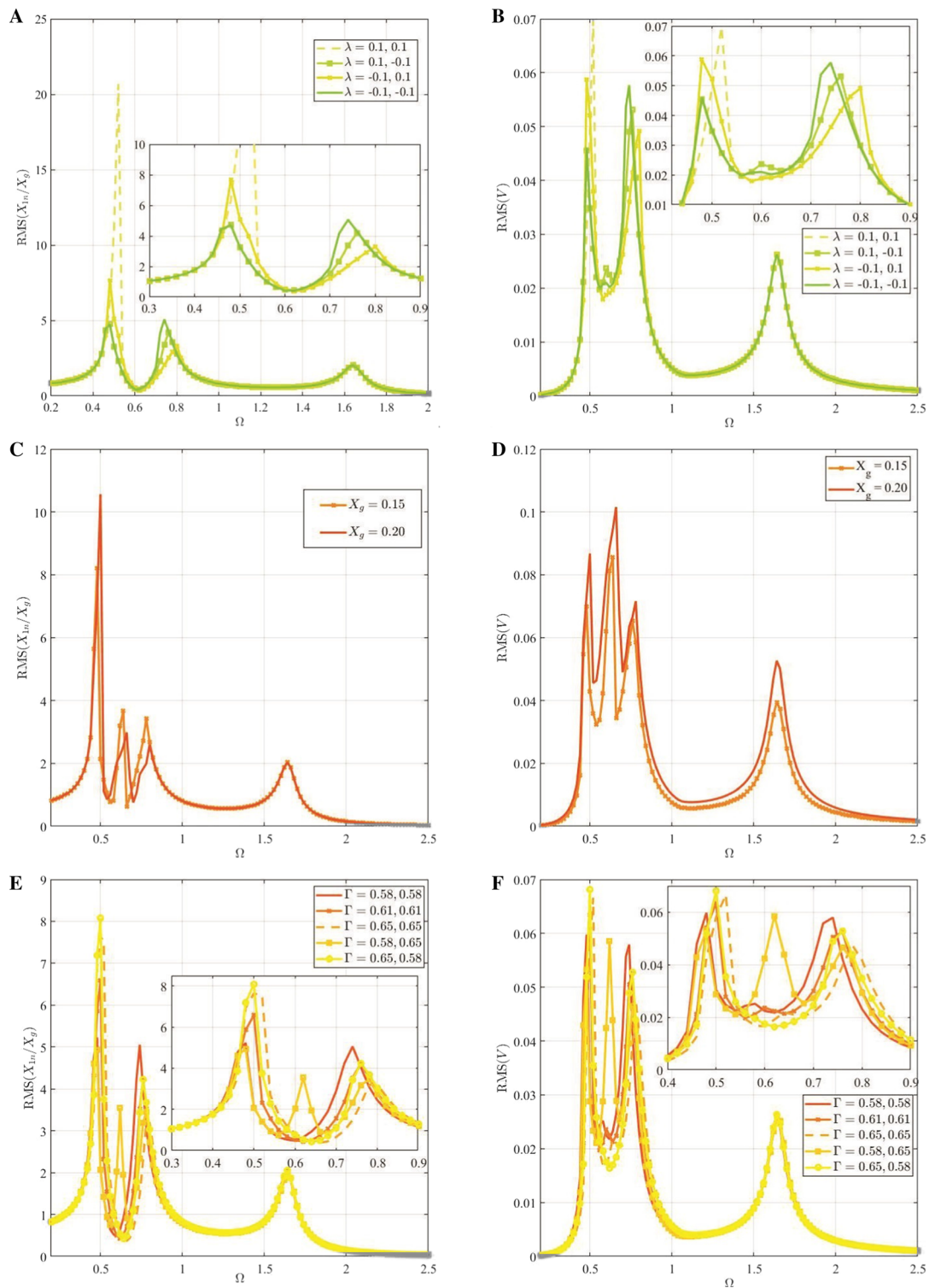
1408

Eur. Phys. J. Spec. Top. (2022) 231:1403–1413

Fig. 3 Dynamic behaviour of 2-cell metamaterial. Considered general non-dimensional parameters are $\zeta_1 = 0.03$, $\zeta_2 = 0.1$, $\mu = 0.2$, $\eta = 1$, $\kappa = \beta = 0.05$. **A** RMS non-dimensional amplitude of first mass versus Ω for different combination of hardening and softening coefficient (λ). **B** Total voltage generated versus Ω for different combination of hardening and softening coefficient (λ). In **A, B** non-dimensional parameters are taken as $X_g = 0.1$ and $\Gamma_{l1} = \Gamma_{l2} = 0.61$. **C** RMS non-dimensional amplitude of first mass versus Ω for differ-

ent X_g. **D** Total voltage generated versus Ω for different X_g **E** RMS non-dimensional amplitude of first mass versus Ω for different combination of linear stiffness coefficient (Γ). **F** Total voltage generated versus Ω for different combination of linear stiffness coefficient (Γ). In **C**–**F**, other non-dimensional parameter are $(\lambda_1 = 0.1, \lambda_2 = -0.1)$. For **C, D** the non-dimensional parameter is taken as $\Gamma_{l1} = \Gamma_{l2} = 0.61$. In **E, F** the non-dimensional parameter is taken as $X_g = 0.1$
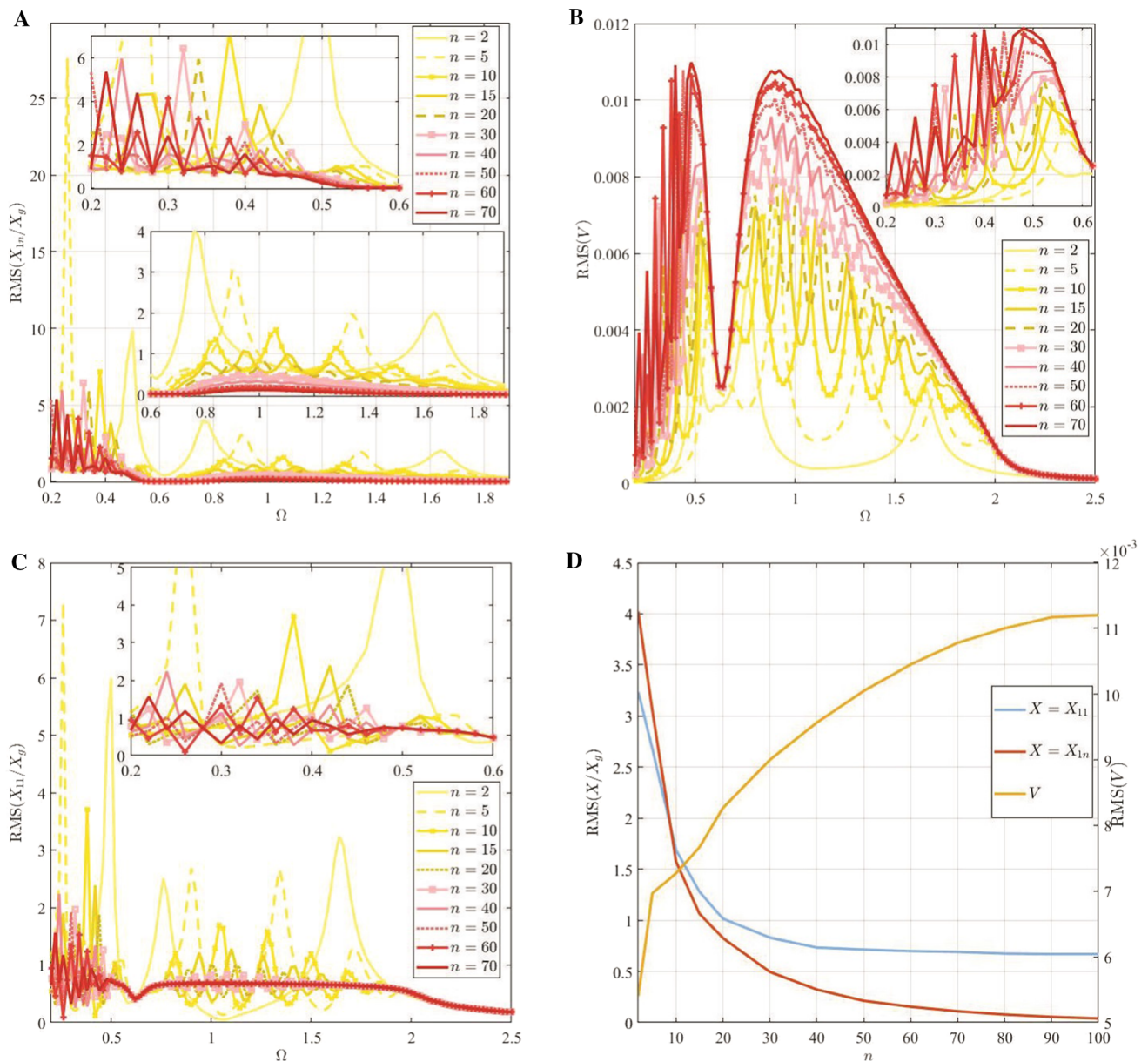
Fig. 4 Dynamic behaviour of multi-cell metamaterial. **A** RMS non-dimensional amplitude of first mass of last unit cell (X_{1n}) versus Ω for different number of unit cell (n). **B** Total voltage generated versus Ω for different number of unit cell (n). **C** RMS non-dimensional amplitude of first mass of first unit cell (X_{11}) versus Ω for different number of unit cell (n). **D** Maximum peak of total voltage, RMS non-dimensional amplitude of first mass and last mass generated versus different number of unit cell (n). The considered non-dimensional parameters are $\zeta_1 = 0.03$, $\zeta_2 = 0.1$, $\mu = 0.2$, $\eta = 1$, $\kappa = \beta = 0.05$, $X_g = 0.01$, $\lambda = 0.1$ and, $\Gamma = 0.61$

amplitude of the first peak is attained. With the introduction of softening effect, we achieve a more favourable response as compared to hardening effect in terms of vibration attenuation. The higher frequency response of the system is independent of the hardening and softening coefficient. For the combination of softening and hardening effect, the softening effect on first unit cell and hardening effect on last unit cell ($\lambda_1 = -0.1$, $\lambda_2 = 0.1$) results in lower first peak, approximately same as the case of both cell having softening coefficient. The hardening effect on the first unit cell and soft-

ening effect on the last unit cell ($\lambda_1 = 0.1$, $\lambda_2 = -0.1$) results in a peak between the purely hardening and softening cases. Thus, providing a softening effect in the first unit cell is more preferable.

Simultaneous energy harvesting from resonators is another intended function of the metastructure. The effects of hardening and softening spring on total voltage are shown in Fig. 3B. For every unit cell, the non-dimensional RMS voltage depends on the relative amplitude of inner and outer mass. Widening the band gap results in more favourable results for energy

1410

Eur. Phys. J. Spec. Top. (2022) 231:1403–1413

harvesting. The numerical results show that the hardening spring configuration obtains higher voltage as compared to the softening spring configuration. For a non-dimensional frequency ($\Omega = 0.6$), we find the same RMS voltage ($V = 0.02$) in every combination of softening and hardening coefficient. In Fig. 3C–F, we present results considering 2-cell systems with hardening effect on the first unit cell and softening effect on last unit cell ($\lambda_1 = 0.1, \lambda_2 = -0.1$). For Fig. 3C, D, the non-dimensional parameter is taken as $\Gamma_{l1} = \Gamma_{l2} = 0.61$. Figure 3C shows the non-dimensional steady-state RMS amplitude of the first mass (m_1) of the last unit cell and Fig. 3D presents the non-dimensional steady-state RMS total voltage for different excitation amplitudes (X_g). It is observed that the non-dimensionless RMS amplitude for higher amplitude excitation is larger for first peak and smaller for other peaks. For higher frequency, responses are less dependent on (X_g). The voltage output increases with the increase in (X_g). Figure 3E represents the non-dimensional steady-state RMS amplitude of first mass (m_1) of last unit cell and Fig. 3F represents the non-dimensional steady-state RMS total voltage for a different combination of linear stiffness coefficient (Γ). For obtaining the results of Fig. 3E, F, we have taken the amplitude as $X_g = 0.1$. It is observed that as Γ increases for both unit cells, the first peak response shows higher amplitude and the second peak shows lower amplitude. A higher value of Γ exhibits the hard spring character, while the lower values represent the soft spring character. The numerical results indicate that the band gap can be maximized for certain combinations of Γ. For example, consideration of $\Gamma = 0.65$ and $\Gamma = 0.58$ for the first and second cells, respectively, results in better band gaps and lower resonating peak.

Figure 4 represents the response of multi-cell metamaterials. The following parameters were used for obtaining the results unless otherwise mentioned: $\zeta_1 = 0.03, \zeta_2 = 0.1, \mu = 0.2, \eta = 1, \kappa = \beta = 0.05, X_g = 0.01, \lambda = 0.1$ and, $\Gamma = 0.61$. Figure 4A presents the RMS non-dimensional amplitude of the first mass of the last unit cell (X_{1n}) versus Ω considering different number of the unit cell (n). Figure 4B shows the total voltage generated versus Ω for different number of unit cells (n). Figure 4C presents RMS non-dimensional amplitude of first mass of the first unit cell (X_{11}) versus Ω for different number of unit cell (n). Figure 4D presents the maximum peak of total voltage along with RMS non-dimensional amplitude of the first mass and the last mass versus different number of the unit cell (n). A general trend is noticed that as the number of unit cell (n) increases, the curves become smoother and last cell amplitude tends to zero. For the first cell, amplitude gets converged to a particular value and Ω does not have significant effect on response up to a reasonably high frequency value. As n increases, total RMS voltage (V) becomes high and the curves become smoother. Thus, increased number of cell shows a favourable outcome for both the vibration attenuation and energy harvesting, but at the expense of having more units and subsequently more material. In the following paragraph,

we further investigate the effect of gradation and other influencing parameters considering a multi-cell metamaterial with a particular value of n.

Figure 5 analyses a multi-cell metamaterial with number of cells as $n = 8$, wherein the effects of functionally varying properties in different unit cells are investigated. Non-dimensional parameters used for obtaining the numerical results of Fig. 5 are $X_g = 0.1$, $\Gamma_{l1} = \Gamma_{l2} = 0.61$, $\zeta_2 = 0.1$, $\eta = 1$, $\kappa = \beta = 0.05$. Considering $\mu = 0.2$ and $\zeta_1 = 0.03$, Fig. 5A, B investigate the effect of varying non-linear stiffness assuming different power-law coefficients (n') as

$$\lambda(i) = 0.2\left(\frac{i-1}{n-1}\right)^{n'} - 0.1 \qquad (10)$$

Figure 5A presents the non-dimensional steady-state RMS amplitude of the first mass (m_1) of the last unit cell and Fig. 5B shows the non-dimensional steady-state RMS total Voltage. For $n' = 0$ all unit cells have $\lambda = 0.1$ and for $n' = \infty$ all unit cell have $\lambda = -0.1$. The λ values are changed by polynomial order (for example $n' = 1$ represents linear variation, $n' = 2$ represents parabolic variation and so on) from $\lambda = 0.1$ for the first unit cell to $\lambda = -0.1$ for the last unit cell. In case of $n' = e$, the λ is varied by exponential order from $\lambda = 0.1$ for the first unit cell to $\lambda = -0.1$ for the last unit cell. The results reveal that the only first peak has a significant impact of varying λ. For all cells having hardening effect, the first peak assumes the largest amplitude, while for all cells having softening effect, the first peak assumes the smallest amplitude.

Figure 5C, D presents the compound influence of Ω and μ on vibration attenuation and energy harvesting considering the non-dimensional parameters as $\zeta_1 = 0.03$ and $\lambda = 0.1$ for all the cells. Figure 5C shows the RMS non-dimensional amplitude of first mass with the coupled variation of Ω and μ, while Figure 5D shows the RMS non-dimensional total voltage with the coupled variation of Ω and μ. As μ increases, the peak amplitude and peak voltage shift towards lower frequency. As Ω increases, the metamaterial obtains a peak of lesser amplitude and after $\Omega = 1.4$ the effect becomes marginal. As Ω increases, the peaks of total voltage increase and subsequently decrease. Furthermore, it is noticed that a smaller value of μ results in a larger total voltage. Figure 5E, F presents the compound influence of Ω and ζ_1 on vibration attenuation and energy harvesting considering the non-dimensional parameters as $\mu = 0.2$ and $\lambda = 0.1$ for all the cells. Figure 5E shows the RMS non-dimensional amplitude of first mass with the coupled variation of Ω and ζ_1, while Fig. 5F shows the RMS non-dimensional total voltage with the coupled variation of Ω and ζ_1. For a lesser value of ζ_1, we observe the multi-valley phenomena and subsequently increase in both the amplitude and voltage is noticed. Thus, for vibration attenuation it is preferable to use larger ζ_1, while a contradictory requirement is found for simultaneously enhancing the energy output.
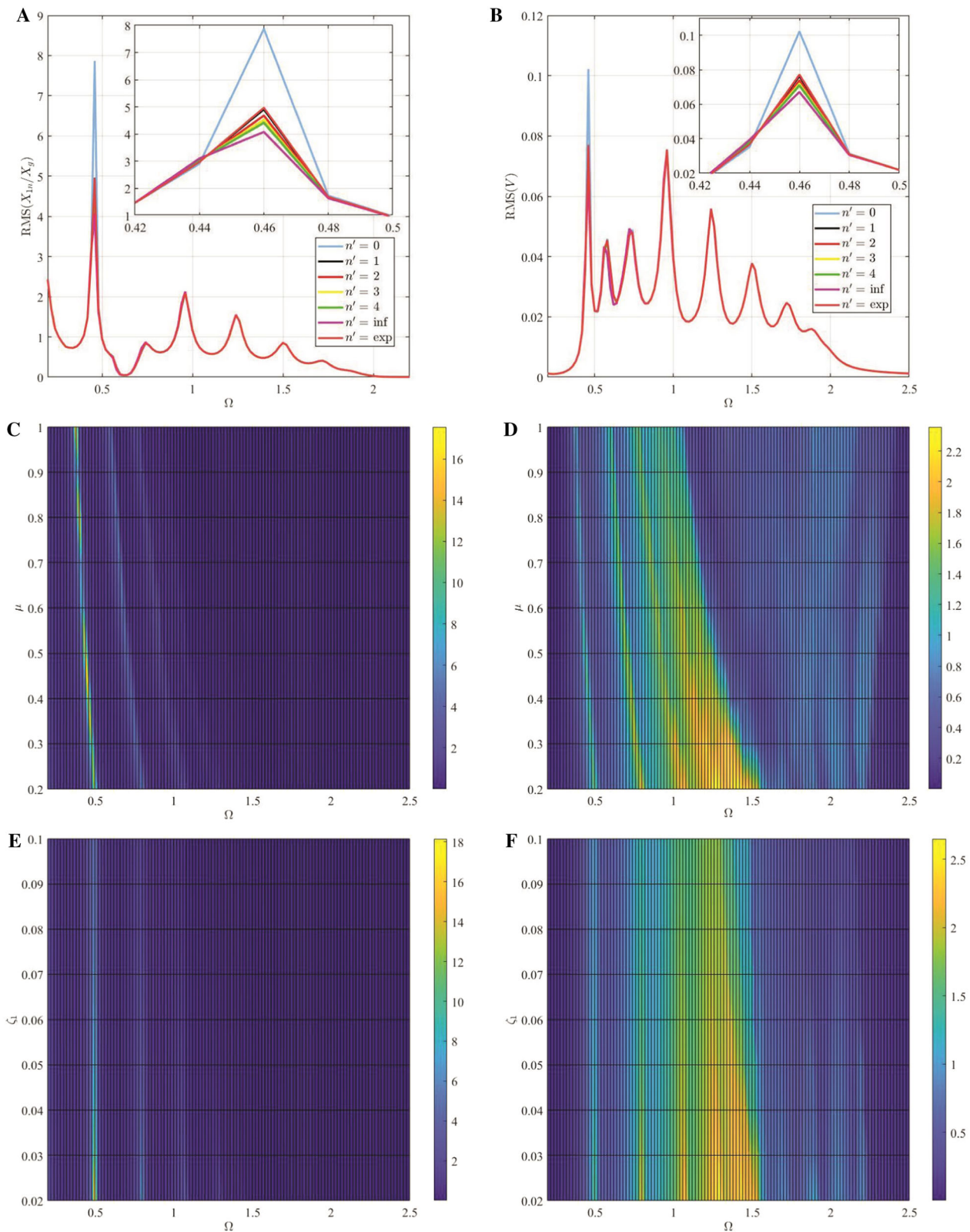
Fig. 5 Effect of different system parameters and gradation on the dynamic behaviours of 8-cell metamaterials. Non-dimensional parameters considered are $X_g = 0.1$, $\Gamma_{l1} = \Gamma_{l2} = 0.61$, $\zeta_2 = 0.1$, $\eta = 1$, $\kappa = \beta = 0.05$. **A** RMS non-dimensional amplitude of first mass versus Ω for different n'. **B** Total voltage generated versus Ω for different n'. In **A, B** the non-dimensional parameters are $\mu = 0.2$, $\zeta_1 = 0.03$. **C** RMS non-dimensional amplitude of first mass versus Ω and μ. **D** Total voltage generated versus Ω and μ. In **C, D** the non-dimensional parameters are $\zeta_1 = 0.03$, $\lambda = 0.1$ for all cells. **E** RMS non-dimensional amplitude of first mass versus Ω and ζ_2. **F** Total voltage generated versus Ω and ζ_2. In **E, F** the non-dimensional parameters are $\mu = 0.2$, $\lambda = 0.1$ for all cells

1412

Eur. Phys. J. Spec. Top. (2022) 231:1403–1413

4 Conclusions and perspective

This paper explores the simultaneous performance of energy harvesting and vibration attenuation of mass-in-mass metamaterials considering multiple unit cells. Based on an analytical approach, we present dimensionless results, revealing the crucial parameters for achieving the dual functionality. In 2-cell metamaterials, our investigation reveals that introducing softening effect gives more vibration attenuation as it decreases the first peak amplitude and hardening effect gives more energy harvesting. Increasing the input vibration amplitude results in enhanced vibration energy, but this also increases the amplitude peak. As we increase the number of unit cells, behavior of system tends to converge to smoother patterns beyond certain numbers. After a critical number of unit cells, the second transmission zone (i.e., $\Omega > 0.6$) completely vanishes and the voltage generation is maximized to a converged level. In a multi-cell metastructure (analysed with 8 cells), introducing non-linearity only impacts on the first peak of vibration amplitude, while for other frequencies, there is negligible effect on vibration attenuation and voltage generation. As we increase μ, voltage and amplitude peaks shift towards the lower frequency, leading to the notion of tuning performance of the metamaterial based on the operational frequency range. It is revealed that the resonant peak can be reduced by non-linear softening characteristics. For enhanced energy harvesting, a smaller value of mass ratio is preferred, while a larger value of damping characteristic is suitable for vibration suppression. Under certain configurations, band structure of the phononic metastructure is capable of achieving absolute band gaps, resulting in frequency ranges, where waves cannot propagate.

In summary, motivated by the elastic negative mass metastructures, this work reports the enhancement of vibration suppression, while achieving better energy harvesting via non-linear attachments. A mathematical model of the functionally graded metastructure having linear spring with nonlinear attachments is developed and analyzed numerically. The comprehensive results presented on the effect of various system parameters including their functional gradation would lead to the design of multi-cell non-linear metamaterials for the dual functionality of vibration attenuation and energy harvesting based on an improved understanding of the physical behaviour.

Declarations

Conflict of interest The authors declare that they have no known competing financial interests or personal relationships that could have appeared to influence the work reported in this paper.

References

1. X.-K. Ge, Q.-X. Zhao, H. Shao, Y. Lu, Research on slenderness structure vibration induced by detouring flow symmetry breaking-taking the accident of tacoma narrow bridge damage caused by wind vibration as an example. J. Disaster Prevent. Mitig. Eng. **31**(4), 430–435 (2011)
2. A.A. Zadpoor, Mechanical meta-materials. Mater. Horizon **3**, 371–381 (2016)
3. T. Mukhopadhyay, S. Adhikari, Stochastic mechanics of metamaterials. Compos. Struct. **162**, 85–97 (2017)
4. T. Mukhopadhyay, S. Adhikari, A. Batou, Frequency domain homogenization for the viscoelastic properties of spatially correlated quasi-periodic lattices. Int. J. Mech. Sci. **150**, 784–806 (2019)
5. T. Mukhopadhyay, J. Ma, H. Feng, D. Hou, J.M. Gattas, Y. Chen, Z. You, Programmable stiffness and shape modulation in origami materials: emergence of a distant actuation feature. Appl. Mater. Today **19**, 100537 (2020)
6. H. Wang, D. Zhao, Y. Jin, M. Wang, T. Mukhopadhyay, Z. You, Modulation of multi-directional auxeticity in hybrid origami metamaterials. Appl. Mater. Today **20**, 100715 (2020)
7. T. Mukhopadhyay, S. Naskar, S. Adhikari, Anisotropy tailoring in geometrically isotropic multi-material lattices. Extreme Mech. Lett. **40**, 100934 (2020)
8. S. Ghuku, T. Mukhopadhyay, Anti-curvature honeycomb lattices for mode-dependent enhancement of nonlinear elastic properties under large deformation. Int. J. Non-Linear Mech. **140**, 103 (2022)
9. T. Mukhopadhyay, D. Kundu, Mixed-mode multidirectional poisson's ratio modulation in auxetic 3d lattice metamaterials. Adv. Eng. Mater. **20**, 2101183 (2021). https://doi.org/10.1002/adem.202101183
10. H.H.C.T. Huang, G.L. Sun, Huang, On the negative effective mass density in acoustic metamaterials. Int. J. Eng. Sci. **47**(4), 610–617 (2009)
11. H.H. Huang, C.T. Sun, Anomalous wave propagation in a one-dimensional acoustic metamaterial having simultaneously negative mass density and young's modulus. J. Acoust. Soc. Am. **132**, 2887–2895 (2012)
12. L. Jensen, C.T. Chan, Double-negative acoustic metamaterial. Phys. Rev. **70**, 055602 (2004)
13. Y. Cheng, J.Y. Xu, X.J. Liu, One-dimensional structured ultrasonic metamaterials with simultaneously negative dynamic density and modulus. Phys. Rev. B **77**, 045134 (2008)
14. Z. Yang, J. Mei, M. Yang, N.H. Chan, P. Sheng, Double-negative acoustic metamaterial. Phys. Rev. **101**, 204301 (2008)
15. S. Adhikari, T. Mukhopadhyay, A. Shaw, N. Lavery, Apparent negative values of young's moduli of lattice materials under dynamic conditions. Int. J. Eng. Sci. **150**, 103231 (2020)
16. T. Mukhopadhyay, S. Adhikari, A. Alu, Theoretical limits for negative elastic moduli in subacoustic lattice materials. Phys. Rev. B **99**, 094108 (2019)

17. T. Mukhopadhyay, S. Adhikari, A. Alu, Probing the frequency-dependent elastic moduli of lattice materials. Acta Mater. **165**, 654–665 (2019)

18. S. Adhikari, T. Mukhopadhyay, X. Liu, Broadband dynamic elastic moduli of honeycomb lattice materials: A generalized analytical approach. Mech. Mater. **157**, 103796 (2021)

19. M. Reynolds, S. Daley, Enhancing the band gap of an active metamaterial. J. Vib. Control **23**(11), 1782–1791 (2017)

20. L. Tang, Y. Yang, A multiple-degree-of-freedom piezoelectric energy harvesting model. J. Intell. Mater. Syst. Struct. **23**, 1631–1647 (2012)

21. H.H. Huang, C.T. Sun, Wave attenuation mechanism in an acoustic metamaterial with negative effective mass density. New J. Phys. **11**, 013003 (2009)

22. M.I. Hussein, M.J. Leamy, M. Ruzzene, Dynamics of phononic materials and structures: Historical origins, recent progress, and future outlook. Appl. Mech. Rev. **66**, 013003 (2014)

23. A.F. Vakakis, O.V. Gendelman, L.A. Bergman, D.M. McFarland, G. Kerschen, Y.S. Lee, *Nonlinear Targeted Energy Transfer in Mechanical and Structural Systems*, vol 156, (Springer Science & Business Media, Berlin, 2008)

24. P. Malaji, M. Rajarathinam, V. Jaiswal, S. Ali, I. Howard, *Energy Harvesting from Dynamic Vibration Pendulum Absorber, Recent Advances in Structural Engineering*, vol 2, (Springer, Berlin, 2019) pp. 467–478

25. A. Banerjee, E.P. Calius, R. Das, Reversible hysteresis for broadband magnetopiezoelastic energy harvesting. Appl. Phys. Lett. **95**, 174103 (2009)

26. H.G.F. Cottone, L. Vocca, Nonlinear energy harvesting. Phys. Rev. Lett. **102**, 080601 (2009)

27. Y. Xia, M. Ruzzene, A. Erturk, Dramatic bandwidth enhancement in nonlinear metastructures via bistable attachments. Appl. Phys. Lett. **114**, 093501 (2019)

28. B.S. Lazarov, J.S. Jensen, Low-frequency band gaps in chains with attached non-linear oscillators. Int. J. Non-Linear Mech. **42**(10), 1186–1193 (2007)

29. Y. Xia, M. Ruzzene, A. Erturk, Bistable attachments for wideband nonlinear vibration attenuation in a metamaterial beam. Nonlinear Dyn. **102**, 1285–1296 (2020)

30. A. Banerjee, E.P. Calius, R. Das, The effects of cubic stiffness nonlinearity on the attenuation bandwidth of 1d elasto-dynamic metamaterials. Am. Soc. Mech. Eng. **2016**, 50671 (2016)

31. G. Chakraborty, A. Mallik, Dynamics of a weakly nonlinear periodic chain. Int. J. Non-Linear Mech. **36**(2), 375–389 (2001)

32. D. Guyomar, A. Badel, E. Lefeuvre, C. Richard, Toward energy harvesting using active materials and conversion improvement by nonlinear processing. IEEE Trans. Ultrason. Ferroelectr. Freq. Control **52**(4), 584–595 (2005)

33. T. Yang, S. Zhou, S. Fang, W. Qin, D.J. Inman, Nonlinear vibration energy harvesting and vibration suppression technologies: designs, analysis, and applications. Appl. Phys. Rev. **8**(3), 031317 (2021)

34. Z. Chen, B. Guo, Y. Yang, C. Cheng, Metamaterials-based enhanced energy harvesting: a review. Phys. B **438**, 1–8 (2014)

35. T. Yang, Q. Cao, Z. Hao, A novel nonlinear mechanical oscillator and its application in vibration isolation and energy harvesting. Mech. Syst. Signal Process **155**, 107636 (2021)

36. A. Singh, T. Mukhopadhyay, S. Adhikari, B. Bhattacharya, Voltage-dependent modulation of elastic moduli in lattice metamaterials: emergence of a programmable state-transition capability. Int. J. Solids Struct. **208–209**, 31–48 (2021)

37. A. Singh, T. Mukhopadhyay, S. Adhikari, B. Bhattacharya, Active multi-physical modulation of poisson's ratios in composite piezoelectric lattices: on-demand sign reversal. Compos. Struct. **280**, 114857 (2022)

38. B.B.D. Moura, M.R. Machado, T. Mukhopadhyay, S. Dey, Dynamic and wave propagation analysis of periodic smart beams coupled with resonant shunt circuits: passive property modulation. Eur. Phys. J. Spec. Top. **2021**, 8 (2022)

39. M. Carrara, M.R. Cacan, J. Toussaint, M.E.M. Leamy, A. Jand-Ruzzene, Metamaterial-inspired structures and concepts for elastoacoustic wave energy harvesting. Smart Mater. Struct. **22**, 065004 (2013)

40. Y. Li, E. Baker, T. Reissman, C. Sun, W.K. Liu, Design of mechanical metamaterials for simultaneous vibration isolation and energy harvesting. Appl. Phys. Lett. **111**(25), 251903 (2017)

41. S. Kumar, N. Naidu, K. Banerjee, T.V.S.R.P. Anil-Babu, A review on metamaterials for device applications. Crystals **11**, 518 (2021)

42. H.A. Sodano, D.J. Inman, G. Park, A review of power harvesting from vibration using piezoelectric materials. Shock Vibr. Digest **36**, 197–206 (2004)

43. L. Tang, Y. Yang, A multiple-degree-of-freedom piezoelectric energy harvesting model. J. Intell. Mater. Syst. Struct. **23**, 1631–1647 (2012)

44. A. Erturk, J. Hoffmann, D.J. Inman, A piezomagnetoelastic structure for broadband vibration energy harvesting. Appl. Phys. Lett. **94**, 254102 (2009)

45. G. Hu, L. Tang, R. Das, Internally coupled metamaterial beam for simultaneous vibration suppression and low frequency energy harvesting. J. Appl. Phys. **123**(5), 055107 (2018)

46. M. Rezaei, R. Talebitooti, W.-H. Liao, Exploiting bistable magneto-piezoelastic absorber for simultaneous energy harvesting and vibration mitigation. Int. J. Mech. Sci. **207**, 106618 (2021)